First Measurement of Near- and Sub-Threshold J/ψ Photoproduction off Nuclei

(Dated: June 24, 2024)

We report on the first measurement of J/ψ photoproduction from nuclei in the photon energy region of $7 < E_\gamma < 10.8$ GeV, extending above and below the threshold energy of $E_\gamma^{th} \sim 8.2$ GeV. The experiment used a tagged photon beam incident on deuterium, helium, and carbon, and the GlueX detector to measure the semi-inclusive $A(\gamma, e^+e^-p)$ reaction with a dilepton invariant mass $M(e^+e^-) \sim m_{J/\psi} = 3.1$ GeV. The incoherent J/ψ photoproduction cross-sections in deuterium, helium, and carbon is measured as a function of the incident photon energy, reconstructed missing light-cone momentum fraction, and momentum transfer. Comparisons with theoretical predictions suggest an excess of the measured cross-section for sub-threshold production and interactions with high missing light-cone momentum fraction.

INTRODUCTION

Understanding the partonic structure of nuclei has been an outstanding question in nuclear physics. Following the discovery of the EMC effect [1–7], it is understood that the partonic structure functions of bound nucleons differ from those of free nucleons. In the decades since this discovery, many high-precision measurements with a large number of nuclei have furthered our knowledge, with particular emphasis on the modification of valance quark distributions in nuclei. Despite several models being able to explain world data, the underlying mechanism driving this modification remains unknown [8–11].

Complementary data probing the gluon structure of the nucleus can help further our understanding of parton dynamics in nuclei. The photoproduction of J/ψ particles off nucleons is mediated primarily by the exchange of gluons, and is therefore directly sensitive to the gluon density inside nucleons. Recent experiments measured the production of J/ψ particles from free protons in the near-threshold energy region [12–14]. These studies have provided the first experimental insights into gluon content of the proton at large momentum-fraction x.

Photoproduction of J/ψ from nuclear targets has the potential to provide similar insights to the gluon content of nuclei and bound nucleons. In particular, the "sub-threshold" photoproduction of J/ψ, using photons with energy below $E_\gamma^{th} \approx 8.2$ GeV, has long been sought after as a signature of high-energy gluon configurations in the nucleus [15–17]. More recently it has been understood that high-energy gluons could largely result from high-momentum nucleons in Short-Range Correlated (SRC) pairs [18, 19]. Sub-threshold production of J/ψ has the potential to be sensitive to a number of exotic effects in nuclei, such as the modification of gluons in SRCs or hidden-color components of the nucleus [20], and is therefore a valuable measurement for our understanding of nuclear structure in extreme conditions.

Few measurements of low-energy J/ψ photoproduction from nuclei have been performed to date [21, 22]. Measuring only the inclusive production of J/ψ, they cannot provide direct knowledge of the incident photon energy. A dedicated search for sub-threshold production of J/ψ has also been made at energies far below threshold, therefore observing no J/ψ events [17].

In this Letter, we present the first measurement of J/ψ production from nuclear targets in the near- and sub-threshold region of $7 < E_\gamma < 10.8$ GeV. These events are identified by the detection of semi-inclusive $A(\gamma, e^+e^-p)$, following the leptonic decay $J/\psi \to e^+e^-$. The detection of a knocked-out proton allows both an improved reconstruction of the dilepton invariant mass and an inference of the initial-state nucleon momentum, allowing an examination of the nuclear effects present in the reaction. We observe a small but significant number of J/ψ events from photons with energy $E_\gamma < 8.2$ GeV, marking the first such observation of sub-threshold J/ψ production. We characterize these events and comment on the implications of the measurement.

EXPERIMENT

The experiment ran in 2021 in Hall D of the Thomas Jefferson National Accelerator Facility. A 10.8 GeV electron beam from the Continuous Electron Beam Accelerator Facility [23] was used to create a tagged linearly-polarized photon beam via coherent bremsstrahlung from a diamond radiator. The energy E_γ of the bremsstrahlung photons follows a spectrum proportional to $1/E_\gamma$, with a primary coherent enhancement at an energy 7.6-8.6 GeV. The photon energy was determined from the momentum of the scattered electron, which was measured in the tagging Microscope and Hodoscope detectors to an accuracy of about 0.1%. This photon beam was collimated upon exiting the tagger hall, after which it is incident on the target within the GlueX spectrometer. The photon flux incident on the target was monitored by the Pair Spectrometer (PS) [24], allowing for a measurement of the energy-dependent luminosity. The experiment used two 30-cm liquid targets, ^{2}H and ^{4}He, with total tagged luminosity of 33 and 60 pb$^{-1}\cdot$ nucleon in the region $E_\gamma > 7$ GeV, respectively. A solid multi-foil ^{12}C target (8 equidistant foils with a total thickness of 1.9 cm, extended over a 30-cm region) was also used, with a total tagged luminosity of 94 pb$^{-1}\cdot$ nucleon in the region $E_\gamma > 7$ GeV.

The GlueX spectrometer [25] is a large-acceptance detector, composed of multiple subdetectors. Immediately surrounding the target is a scintillator-based start counter (SC) [26], followed by a straw-tube central drift chamber (CDC) [27], a lead and scintillating-fiber barrel calorimeter (BCAL) [28], and a superconducting solenoid magnet. Further downstream in the direction of the beamline are a set of planar wire forward drift chambers (FDC) [29], a time-of-flight scintillator detector (TOF), and a lead-glass forward calorimeter (FCAL) [30]. Events were recorded when either sufficient deposition of energy in the calorimeters, or a lesser energy deposition paired with a hit in the SC was measured.

We study the semi-inclusive reaction $\gamma A \to e^+e^-p(X)$, where X denotes the undetected residual nuclear state. The charged particles in this reaction were measured in the drift chambers, with their tracks in the magnetic field used to determine their momentum. Other sub-detectors were used for particle-identification. Tracking resolution was improved utilizing a kinematic fit constraining a common reaction vertex in the target for all measured tracks.

The identification of electrons and rejection of pion backgrounds was performed using two calorimetry method following Ref. [12, 14]. First, selections were applied on the momentum-energy ratio p/E, where the charged particle momentum p was determined using the charged track information from the drift chambers, and the energy E was determined from the energy deposition in the calorimeters. Because electrons and positrons deposit the majority of their energy in the calorimeters, in contrast to heavier particles, this value is expected to be close to 1. As in previous studies, this ratio was constrained to $-3\sigma < p/E - \langle p/E\rangle < 2\sigma$, where σ is the resolution on p/E in each calorimeter, found to be 8% for the FCAL and 7% for the BCAL. These resolutions differ somewhat from those previously measured in GlueX, primarily due to their use of a hydrogen target that allowed utilizing an exclusivity requirement in the kinematic fit, resulting in further improved momentum resolution. The second method of e/π separation used the innermost layer of the BCAL as a preshower detector, requiring the energy E_{pre} deposited in this layer by a lepton candidate to satisfy $E_{pre}\sin\theta > 30$ MeV, where the sine of the charged particle angle θ accounts for the path length of the particle in the BCAL layer. As electrons and positrons deposit much more energy in this layer than pions, this selection cut also rejects a large fraction of the pion backgrounds. Identification of the proton in the reaction was performed by the combination of the measured particle momentum from the drift chambers and measurements of the particle time-of-flight from the FCAL, BCAL, or TOF, as well as energy loss in the drift chambers and SC.

Tagged beam photons were associated with an event if they fell within 2 ns of the tagged beam bunch RF time. To account for the substantial rate of accidental photons in the tagger, off-time photons between 6 and 18 ns before or after the RF time of the event were taken as a measurement of the photon pileup to be subtracted from the data via event-mixing.

Additional cuts were applied on the events to improve signal-to-background ratios. All charged particles were required to have a momentum > 0.4 GeV/c, as well as a polar angle $> 2°$, in order to stay within the fiducial region of the detector where the acceptance and response are modeled well. The vertex of the event was required to fall within the volume of the target. An "elasticity" requirement was also placed on the events, requiring energy balance within 1 GeV between the initial- and final-state particles assuming scattering from a quasi-free proton. Finally, events with extra tracks in the drift chambers or showers in the calorimeters were removed.

The J/ψ yield was determined by examining the invariant mass spectrum of the final-state dilepton. The poor dilepton invariant mass reconstruction resolution substantially reduced our ability to isolate J/ψ signal over background, resulting from residual $\pi^+\pi^-$ pion misidentification and Bethe-Heitler e^+e^- production. To improve on this, we make the observation that, along with the transverse momentum $p_\perp$, the light-cone coordinate "minus" component of momentum $p^- \equiv E - p_z$ is well-reconstructed for the high-momentum leptons, where E and p_z are the energy and longitudinal component of momentum relative to the beamline. Combining this with the fact that the low-momentum proton and tagged photon are well-reconstructed, we may make the approximation of quasi-elastic J/ψ production from a standing pair of nucleons, with the assumption that the initial momentum of the struck nucleon is balanced by a single partner in the final state. Under this approximation, we calculate the dilepton mass using well-measured quantities:

$$\begin{aligned} m^2(e^+e^-) &\approx m^2_{\text{light-cone}} \\ &= \left(p^-_{e^+} + p^-_{e^-}\right)\left(2E_\gamma + 2m_N - p^+_p - \frac{m_N^2 + p^2_{\text{tot}}}{2m_N - p^-_{\text{tot}}}\right) \\ &\quad - \left(\vec{p}^{\,\perp}_{e^+} + \vec{p}^{\,\perp}_{e^-}\right)^2 . \end{aligned} \tag{1}$$

where m_N is the nucleon mass, $p^+ \equiv E - p_z$ is the "plus" component of momentum, and $p_{\text{tot}} = p_{e^+} + p_{e^-} + p_p$ is the total momentum of the measured final-state. This "light-cone" mass proxy allows substantially improved resolution and the isolation of J/ψ events above background. Figure 1 shows the $m_{\text{light-cone}}$ distribution for the combined data of all targets. The peak resulting from the $J/\psi \to e^+e^-$ decay can be clearly seen. The insert shows the same for events in the "sub-threshold" region $E_\gamma < 8.2$ GeV, where we also observe the $J/\psi \to e^+e^-$ decay peak resulting from sub-threshold production of J/ψ. For the absolute cross sections, the yields were determined by performing an unbinned likelihood fit on the light-cone mass assuming an exponential background.

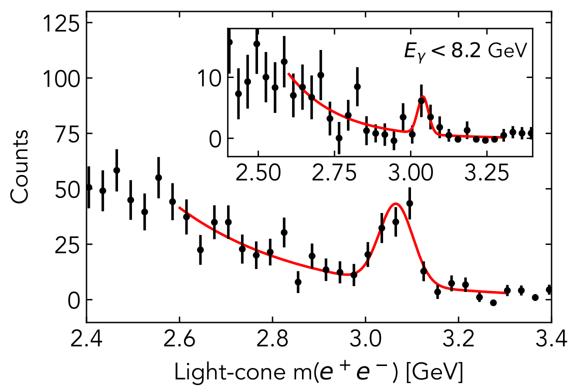

FIG. 1. *Main figure:* Light-cone mass distribution for the combined data of all targets, fit using an exponential background and a Gaussian signal. *Insert:* Light-cone mass distribution for events in the "sub-threshold" region $E_\gamma < 8.2$ GeV. In both cases the J/ψ decay can be clearly seen.

For the differential cross sections, the yields were determined by performing side-band subtraction using the region $2.7 < m_{\text{light-cone}} < 3.4$ GeV as a measure of the background contribution.

We performed Monte Carlo simulation of quasi-elastic J/ψ production from ^{2}H, ^{4}He, and ^{12}C, in order to compare with distributions in data as well as estimate the event detection efficiency. The quasi-elastic process $(\gamma, J/\psi p)$ was simulated using a factorized cross section model in the Plane-Wave Impulse Approximation (PWIA):

$$\frac{d\sigma(\gamma A \to J/\psi pX)}{dt d^3\vec{p}_i dE_i} = v_{\gamma i} \cdot \frac{d\sigma}{dt}(\gamma p \to J/\psi p) \cdot S(p_i, E_i) \quad (2)$$

where $p_i = (E_i, \vec{p}_i)$ is the 4-momentum of the struck proton i inside the nucleus, p_γ is the 4-momentum of the incoming beam photon, $v_{\gamma i} = p_\gamma \cdot p_i/(E_\gamma E_i)$ is the relative velocity between the photon and the struck proton, and the differential cross section $d\sigma/dt$ for the exclusive process $(\gamma p \to J/\psi p)$ was taken from a fit to GlueX data [14]. The spectral functions $S(p_i, E_i)$ for helium and carbon were provided by Ref. [31] for mean-field protons and the Generalized Contact Formalism [32–34] for the SRC protons, calculated using the phenomenological AV18 interaction [35]. The momentum distribution for deuterium was taken from Ref. [36], again calculated using the AV18 interaction. The produced J/ψ was assumed to decay to e^+e^- in a helicity-conserving manner.

The generated PWIA events were simulated using the GEANT model of the GlueX detector [25], and reconstructed as measured data. This simulated detector response was superimposed with randomly triggered samples of data during the run, in order to account for photon tagger accidentals and detector pileup. These simulations were used to extract the reconstruction efficiency for $J/\psi p$ events, found to be $\sim$13% with little variation as a function of beam photon energy or nucleus. Following a recent study of the QED Bethe-Heitler process with GlueX [37], the simulation extracted efficiency was rescaled by a factor of $0.847 \pm 0.019\%$, accounting for simulation imperfections and resulting in an estimated average efficiency of $\sim$11%.

RESULTS

We calculate the total cross section as a function of the incoming photon energy using the following formula:

$$\sigma(E_\gamma) = \frac{Y_{J/\psi}(E_\gamma)}{\mathcal{L}(E_\gamma)\epsilon(E_\gamma)T_A\mathcal{B}(J/\psi \to e^+e^-)}. \quad (3)$$

Here $Y_{J/\psi}$ is the extracted yield of $J/\psi \to e^+e^-$ decays, $\mathcal{L}$ is the tagged photon luminosity, ϵ is the reconstruction efficiency as determined from Monte-Carlo simulations, T_A is the proton transparency for nucleus A, and $\mathcal{B}(J/\psi \to e^+e^-) \approx 5.97 \pm 0.03\%$ is the branching fraction of J/ψ into e^+e^- [38].

Point-to-point systematic uncertainties were calculated for several sources. The dominant uncertainty results from the dependence of the extracted cross section on the selection cuts, determined by varying the values of the lepton PID and energy balance cuts and then taking the resulting variance on the extracted cross section. Also considered was uncertainty in the energy-dependence of the measured luminosity resulting from the acceptance of the PS, uncertainty in the efficiency as a function of final-state kinematics, and uncertainty on the method used to extract the J/ψ yield.

Normalization uncertainty was also determined for each nucleus, ranging from a total of 20% to 24%. This uncertainty is dominated by the uncertainty on the Monte-Carlo efficiency calculations; Ref. [37] estimated a 19.5% uncertainty using Bethe-Heitler and simulation to benchmark the exclusive measurement $\gamma p \to J/\psi p$, and we refer to this estimate. Further normalization uncertainty results from value of the proton transparency as well as uncertainty on target thickness and density.

Table I lists the total cross section for each nucleus, averaged over the photon flux for each target, comparing

TABLE I. Total per-proton cross sections for A$(\gamma, J/\psi p)X$ luminosity-averaged over the energy range $7 < E_\gamma < 10.6$ GeV. Data also includes a common 19.5% normalization uncertainty (not shown).

Nucleus	Plane-wave cross section	Measured cross section	Statistical uncertainty	Systematic uncertainty
^{2}H	0.24 nb	0.23 nb	0.07 nb	0.04 nb
^{4}He	0.22 nb	0.33 nb	0.06 nb	0.05 nb
^{12}C	0.24 nb	0.25 nb	0.05 nb	0.05 nb

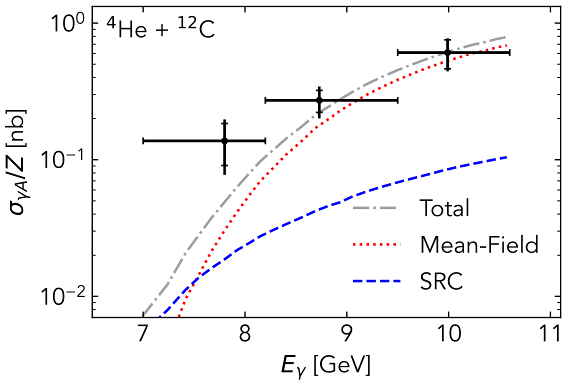

FIG. 2. Luminosity-weighted average of the A($\gamma, J/\psi p$)X cross section for ^{4}He and ^{12}C, compared with plane-wave calculations for this average. The measured cross section (black) is compared with plane-wave calculations, including the mean-field (dotted red) and SRC (dashed blue) contributions as well as the total (dot-dashed grey). Data also includes a common 23% normalization uncertainty (not shown).

the plane-wave calculations with the measured data. In Figure 2 we show instead the energy-dependence of the cross sections for ^{4}He and ^{12}C, where the result has been combined in a yield-weighted fashion to improve the statistical precision, and compare the data with plane-wave calculations which separate the contribution from mean-field and short-range correlated nucleons. We observe that both the A-dependence and the energy-dependence of the measured cross sections are largely consistent with the predictions of plane-wave calculations. We find that we are able to measure the cross section in the sub-threshold energy region $E_\gamma < 8.2$ GeV, marking the first such measurement of J/ψ production below the proton energy threshold. The sub-threshold cross section appears to exceed the plane-wave predictions, indicating the possibility of more exotic mechanisms at play, but uncertainties are large in this region.

In order to further understand the nuclear effects present in the reaction, we examine the differential cross section as a function of the struck proton "missing" 4-momentum

$$p_{\rm miss} = p_{e^+} + p_{e^-} + p_p - p_\gamma \,, \tag{4}$$

specifically examining the "light-cone momentum fraction"

$$\alpha_{\rm miss} = \frac{E_{\rm miss} - p_{z,{\rm miss}}}{m_A/A} \tag{5}$$

of the proton, which gives a measure of the internal nuclear momentum and is well-measured in the GlueX spectrometer. Figure 3 shows the differential cross section, extracted separately in the sub-threshold energy region $7 < E_\gamma < 8.2$ GeV and the above-threshold energy region $8.2 < E_\gamma < 10.6$ GeV. The data are compared with

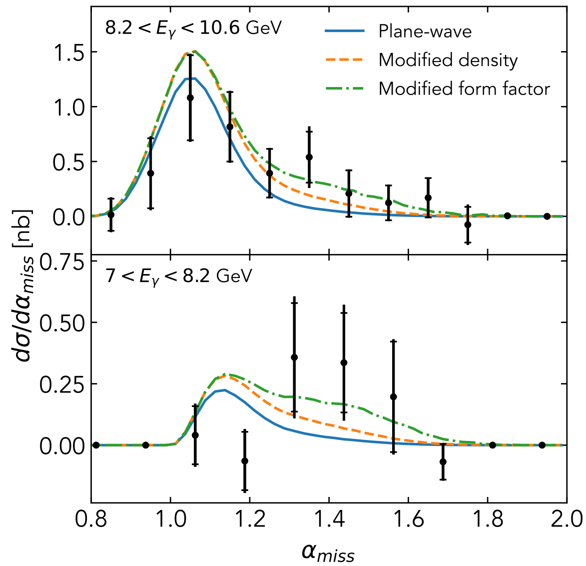

FIG. 3. Differential A($\gamma, J/\psi p$)X cross section as a function of light-cone momentum fraction $\alpha_{\rm miss}$, separated into the above-threshold (top) and below-threshold (bottom) energy regions. Measured data (black points) are compared with plane-wave calculations (blue solid line), as well as calculations assuming a modified proton density (orange dashed) and a modified form factor (green dot-dashed). Data also includes a common 23% normalization uncertainty (not shown).

the plane-wave calculations. In the above-threshold region, the data largely agree with predictions, but the sub-threshold data show greater disagreement. In the sub-threshold region the contribution from large-$\alpha_{\rm miss}$ events is greater than expected, indicating that high-momentum, deeply-bound nucleons contribute more to the J/ψ cross section than anticipated.

We consider two possible mechanisms by which the cross section for which deeply-bound protons might be modified, in both cases depending on the "virtuality" $v = (p_i^2 - m_N^2)/m_N^2$ of the bound proton, which quantifies the degree to which the bound proton proton is off the mass shell and is hypothesized to induce modification of nucleon structure [39]. The first hypothesis is that the overall scale of the cross section is increased as a function of virtuality, meaning that bound protons couple more strongly to the J/ψ. The second hypothesis is that the t-dependence of the cross section is modified, manifesting as a decrease in the slope of the effective form factor for bound protons. The former implies an increase in the effective gluon density of the bound proton, while the latter implies a decrease in the effective gluon radius. Both of these models are shown in Figure 3; specific details are given in the Supplemental Material. In both cases the modification to the photon-proton cross section results in an overall increase of the photon-nucleus cross section. The modification to the form factor predicts a greater increase of the cross section at large α_{miss}, and is preferred by the data over the plane-wave, but the precision of the current data is insufficient to clearly distinguish between the hypotheses.

Other possible exotic production mechanisms could cause an enhancement in the cross section below threshold. One possibility is a contribution from hidden-color components of the nucleus, which would enhance coupling via multi-gluon exchanges, as shown in Fig. 4 of Ref [20]. Other possible mechanisms include intrinsic charm components of the nucleus, strong binding effects of the J/ψ in cold nuclear matter, or non-local production of $c\bar{c}$ in an extended region of the nucleus. A more precise measurement of sub-threshold production of J/ψ is called for in order to place more stringent limits on such exotic effects.

CONCLUSIONS

In conclusion, we report on the first measurement of J/ψ photoproduction from nuclei at and below the energy threshold of 8.2 GeV. We measure threshold J/ψ cross-section for several light nuclei and observe no substantial A-dependence. We extract the energy-dependent cross section for J/ψ production from light nuclei ^{4}He and ^{12}C and compare with plane-wave predictions for near- and sub-threshold production. In the sub-threshold region, we observe J/ψ production for the first, and note an excess production relative to theoretical predictions. We examine the kinematic distributions of these events and note the sensitivity of sub-threshold J/ψ to modified gluon structure in deeply bound nucleons.

We acknowledge the efforts of the staff of the Accelerator and Physics Divisions at Jefferson Lab that made this experiment possible. We thank the staff of Jefferson Lab Hall D and many members of the GlueX collaboration for their support of this experiment and their efforts in developing the detector and the analysis tools used here. This work was supported in part by the U.S. Department of Energy, the U.S-Israel Binational Science Foundation, and the Israel Science Foundation. Jefferson Science Associates operates the Thomas Jefferson National Accelerator Facility for the DOE, Office of Science, Office of Nuclear Physics under contract DE-AC05-06OR23177. This research also used resources of the National Energy Research Scientific Computing Center (NERSC), a U.S. Department of Energy Office of Science User Facility operated under Contract No. DE-AC02-05CH11231. This research was supported in part by Lilly Endowment Inc., through its support for the Indiana University Pervasive Technology Institute.

[1] R. G. Arnold *et al.*, Measurements of the a dependence of deep-inelastic electron scattering from nuclei, Phys. Rev. Lett. **52**, 727 (1984).
[2] J. Aubert *et al.*, Phys. Lett. B **123**, 275 (1983).
[3] J. Ashman *et al.*, Measurement of the ratios of deep inelastic muon-nucleus cross sections on various nuclei compared to deuterium, Phys. Lett. B **202**, 603 (1988).
[4] J. Gomez *et al.*, Measurement of the A dependence of deep-inelastic electron scattering, Phys. Rev. D **49**, 4348 (1994).
[5] M. Arneodo *et al.*, Measurements of the nucleon structure function in the range $0.002 < x < 0.17$ and $0.2 < Q^2 < 8$ GeV^2 in deuterium, carbon and calcium, Nucl. Phys. B **333**, 1 (1990).
[6] J. Seely *et al.*, New Measurements of the European Muon Collaboration Effect in Very Light Nuclei, Phys. Rev. Lett. **103**, 202301 (2009).
[7] B. Schmookler *et al.* (CLAS Collaboration), Modified structure of protons and neutrons in correlated pairs, Nature **566**, 354 (2019).
[8] L. Frankfurt and M. Strikman, Hard nuclear processes and microscopic nuclear structure, Phys. Rep. **160**, 235 (1988).
[9] M. M. Sargsian *et al.*, Hadrons in the nuclear medium, J. Phys. **G29**, R1 (2003).
[10] P. R. Norton, The EMC effect, Reports on Progress in Physics **66**, 1253 (2003).
[11] O. Hen *et al.*, Nucleon-Nucleon Correlations, Short-lived Excitations, and the Quarks Within, Rev. Mod. Phys. **89**, 045002 (2017).
[12] A. Ali *et al.* (GlueX Collaboration), First Measurement of Near-Threshold J/ψ Exclusive Photoproduction off the Proton, Phys. Rev. Lett. **123**, 072001 (2019).
[13] B. Duran *et al.*, Determining the gluonic gravitational form factors of the proton, Nature **615**, 813 (2023).
[14] S. Adhikari *et al.* (GlueX Collaboration), Measurement of the J/ψ photoproduction cross section over the full near-threshold kinematic region, Phys. Rev. C **108**, 025201 (2023).
[15] P. Hoyer, Physics at ELFE, Nuclear Physics A **622**, c284 (1997).
[16] P. Hoyer, Charmonium Production at ELFE Energies (1997), arXiv:hep-ph/9702385 [hep-ph].
[17] P. Bosted *et al.*, Search for sub-threshold photoproduction of J/ψ mesons, Phys. Rev. C **79**, 015209 (2009).
[18] J. Xu and F. Yuan, Gluonic probe for the short range correlation in nucleus, Physics Letters B **801**, 135187 (2020).
[19] Y. Hatta *et al.*, Sub-threshold J/ψ and Υ production in γA collisions, Physics Letters B **803**, 135321 (2020).
[20] S. Brodsky *et al.*, Photoproduction of charm near threshold, Physics Letters B **498**, 23 (2001).
[21] B. Gittelman *et al.*, Photoproduction of the $\psi(3100)$ Meson at 11 GeV, Phys. Rev. Lett. **35**, 1616 (1975).
[22] U. Camerini *et al.*, Photoproduction of the ψ particles, Phys. Rev. Lett. **35**, 483 (1975).
[23] C. W. Leemann *et al.*, THE CONTINUOUS ELECTRON BEAM ACCELERATOR FACILITY: CEBAF at the Jefferson Laboratory, Annual Review of Nuclear and Particle Science **51**, 413 (2001), https://doi.org/10.1146/annurev.nucl.51.101701.132327.

[24] F. Barbosa *et al.*, Pair spectrometer hodoscope for Hall D at Jefferson Lab, Nuclear Instruments and Methods in Physics Research Section A: Accelerators, Spectrometers, Detectors and Associated Equipment **795**, 376 (2015).

[25] S. Adhikari *et al.*, The GlueX beamline and detector, Nuclear Instruments and Methods in Physics Research Section A: Accelerators, Spectrometers, Detectors and Associated Equipment **987**, 164807 (2021).

[26] E. Pooser *et al.*, The GlueX Start Counter Detector, Nuclear Instruments and Methods in Physics Research Section A: Accelerators, Spectrometers, Detectors and Associated Equipment **927**, 330 (2019).

[27] N. Jarvis *et al.*, The Central Drift Chamber for GlueX, Nuclear Instruments and Methods in Physics Research Section A: Accelerators, Spectrometers, Detectors and Associated Equipment **962**, 163727 (2020).

[28] T. Beattie *et al.*, Construction and performance of the barrel electromagnetic calorimeter for the GlueX experiment, Nuclear Instruments and Methods in Physics Research Section A: Accelerators, Spectrometers, Detectors and Associated Equipment **896**, 24 (2018).

[29] L. Pentchev *et al.*, Studies with cathode drift chambers for the GlueX experiment at Jefferson Lab, Nuclear Instruments and Methods in Physics Research Section A: Accelerators, Spectrometers, Detectors and Associated Equipment **845**, 281 (2017).

[30] K. Moriya *et al.*, A measurement of the energy and timing resolution of the GlueX Forward Calorimeter using an electron beam, Nuclear Instruments and Methods in Physics Research Section A: Accelerators, Spectrometers, Detectors and Associated Equipment **726**, 60 (2013).

[31] N. Rocco and A. Lovato, private communication.

[32] R. Weiss *et al.*, Energy and momentum dependence of nuclear short-range correlations - Spectral function, exclusive scattering experiments and the contact formalism, Phys. Lett. **B791**, 242 (2019), arXiv:1806.10217 [nucl-th].

[33] A. Schmidt *et al.* (CLAS), Probing the core of the strong nuclear interaction, Nature **578**, 540 (2020), arXiv:2004.11221 [nucl-ex].

[34] J. Pybus *et al.*, Generalized contact formalism analysis of the ^{4}He$(e, e'pN)$ reaction, Phys. Lett. B **805**, 135429 (2020), arXiv:2003.02318 [nucl-th].

[35] S. Veerasamy and W. N. Polyzou, Momentum-space Argonne V18 interaction, Phys. Rev. C **84**, 034003 (2011).

[36] R. B. Wiringa *et al.*, Nucleon and nucleon-pair momentum distributions in $A \leq 12$, Phys. Rev. C **89**, 024305 (2014).

[37] S. Adhikari *et al.*, Search for photoproduction of axionlike particles at GlueX, Physical Review D **105**, 10.1103/physrevd.105.052007 (2022).

[38] R. L. Workman *et al.* (Particle Data Group), Review of Particle Physics, PTEP **2022**, 083C01 (2022).

[39] G. A. Miller, Confinement in nuclei and the expanding proton, Physical Review Letters **123**, 10.1103/physrevlett.123.232003 (2019).